# *In vivo* Prediction of Spermatogenesis in Seminiferous Tubules using High-Resolution Magnetic Resonance Imaging and Machine-Learning Techniques in Combination

**M. Yamaguchi[1], N. Kutsuna[2,3], R. Nakagami[1,4], A. Nabetani[5], A. Nozaki[5], M. Niitsu[4], S. Hasezawa[2,3], and H. Fujii[1,3]**

[1]Functional Imaging Division, National Cancer Center Hospital East, Kashiwa, Chiba, Japan, [2]Graduate School of Frontier Sciences, University of Tokyo, Kashiwa, Chiba, Japan, [3]Institute for Bioinformatics Research and Development-Japan Science and Technology Agency, Chiyoda, Tokyo, Japan, [4]Graduate School of Human Health Sciences, Tokyo Metropolitan University, Arakawa, Tokyo, Japan, [5]GE Healthcare Japan, Hino, Tokyo, Japan

**Introduction:** Recent advances in reproductive technology have brought hope of having a child to infertile men. Testicular sperm extraction (TESE) is an effective method that recovers intratesticular sperm from a small fragment of seminiferous tubules excised under microscopic surgery, followed by artificial fertilization. To increase the sperm retrieval rate in TESE, a navigation system that shows surgeons which seminiferous tubules are possibly producing sperm would be helpful. Our ultimate goal is to construct such a navigation system using high-resolution (HR) MRI and a machine-learning technique in combination; however, the aim of this preliminary study is to demonstrate the feasibility of these techniques for the differentiation of seminiferous tubules with normal and impaired spermatogenesis using an animal model.

**Materials and methods:** MR images were acquired with a 3 Tesla whole-body scanner (Signa HDx; GE, Milwaukee, WI) equipped with a dedicated small coil (solenoid type, 35 mm in diameter, 3 turns). All animal experiments were conducted according to the protocol approved by the institutional review board. Male rats (n=4) were administered a single dose of doxorubicin (DOX, 6mg/kg body weight). Another group of rats (n=4) was administered an equivalent volume of normal saline and served as a control. At 4 and 8 weeks after administration, HR spin echo images of the testis were obtained with a repetition time of 4000 ms, echo time of 90 ms, and resolution of 78 x 78 x 1000μm$^3$. The acquisition time was 13.5 min. We evaluated the testicular volume and the findings of seminiferous tubules. After the MRI scan, testicles were excised and fixed with formalin acetate solution. Histological specimens of the testicles were stained with hematoxylin and eosin (HE). Seminiferous tubular diameter (STD) was microscopically assessed on specimens by calculating the average diameter of 10 representative seminiferous tubules under 100 times magnification. Automatic classification was performed based on supervised learning using in-house software as follows [1]; 1. Two hundred and seven, 103, and 43 regions-of-interest (ROIs, 312 x 312μm$^2$ ) were placed on MR images of the testes of the control, and 4 and 8 weeks after DOX administration, respectively (Fig. 1a). These ROIs were assigned as group 1 (normal spermatogenesis), 2 (mild spermatogenic impairment), and 3 (severe spermatogenic impairment), respectively. 2. After normalization of signal intensities in these ROIs, 186 statistically-relevant features were automatically measured. Of these 186, 16, including perimeters of the contiguous gray-white interfaces along MR visible fine structures (possibly seminiferous tubules), were selected as the best set to classify these three groups (Fig. 1e). 3. A self-organizing map based on these 16 features was drawn to determine the efficacy of the classification (Fig. 1f). Finally, eight-fold cross-validation analysis was performed to confirm the accuracy of the classification.

**Fig. 1**

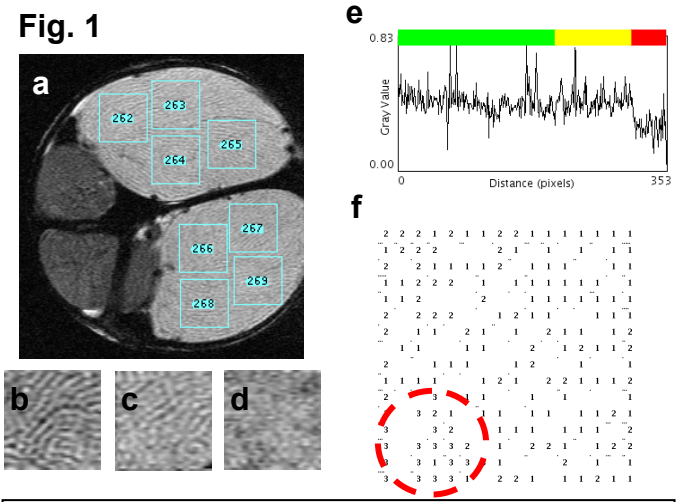


Fig. 1a shows HR MRI of the normal rat testis and ROIs analyzed using machine-learning technique. Fig. 1b–d demonstrate typical findings of the seminiferous tubules in the control (b), and 4 weeks (c) and 8 weeks (d) after DOX administration. A plot (e) shows the perimeter of the contiguous gray-white interfaces along the MR visible fine structures clearly differentiates ROIs with normal (colored green) and mildly impaired (yellow) spermatogenesis from severely impaired spermatogenesis (red). A self-organizing map (f) clearly differentiates group 3 (severely impaired spermatogenesis by DOX) from the other 2 groups.

**Results:** The estimated testicular volumes were 1.04 ± 0.07g, 0.69 ± 0.09g, and 0.33 ± 0.10g before, and at 4 and 8 weeks after DOX administration, respectively. These were 1.12 ± 0.07g, 1.25 ± 0.11g, and 1.12 ± 0.26g, respectively, in the control. The difference between DOX and control groups were statistically significant ($p<0.01$, Bonferroni test). The seminiferous tubules were clearly visualized as tubular structures with high signal lumens and low signal walls in the control and in rats 4 weeks after DOX administration (Fig. 1b and c) [2]; however, they were obscured in rats 8 weeks after DOX administration (Fig. 1d). STD values were 141 ± 6 and 230 ± 24μm 8 weeks after DOX administration and in the control, respectively ($p<0.01$, t-test). Automatic classification showed 85% overall accuracy in classifying the three groups (90.3%, 72.8%, and 86.0% in the control, and mild and severe spermatogenic impairment groups, respectively). The positive predictive value was 76.6% for normal spermatogenesis.

**Discussion:** The reduction in testicular volume and STD values indicate that spermatogenesis is mildly and severely impaired depending on the duration after DOX administration. Thin seminiferous tubules 8 weeks after DOX administration were not clearly visualized on *in vivo* MRI suggesting that the individual measurement of STD on *in vivo* MRI is not realistic. Instead, the machine-learning method used here evaluates ROIs containing dozens of seminiferous tubules as a whole and successfully differentiates those with mild and severe spermatogenetic impairment by DOX and under normal conditions.

**Conclusion: The combination of HR MRI and machine-learning techniques is promising for the prediction for spermatogenesis in seminiferous tubules.**

References: [1] Gambe AE, et al. Cytometry Part A 2007: 71A;286–291 [2] Yamaguchi M, et al. MRM 2009:62:637–644

Acknowledgement: This study was supported by Grant-in-Aid for Scientific Research (KAKENHI) #19890281 from the Ministry of Education, Culture, Sports and Technology and Japan society for the Promotion of Science and Institute for Bioinformatics Research and Development-Japan Science and Technology Agency.